

The Effect of Mean Stress on Damage Predictions for Spectral Loading of Fiberglass Composite Coupons¹

Herbert J. Sutherland
Sandia National Laboratories
Albuquerque, NM 87185-0708
hjsuthe@sandia.gov

John F. Mandell
Montana State University
Bozeman, MT 59717
johnm@coe.montana.edu

Abstract:

In many analyses of wind turbine blades, the effects of mean stress on the determination of damage in composite blades are either ignored completely or they are characterized inadequately. Mandell, et al [1] have recently presented an updated Goodman diagram for a fiberglass material that is typical of the materials used in wind turbine blades. Their formulation uses the MSU/DOE Fatigue Data Base [2] to develop a Goodman diagram with detailed information at thirteen R-values. Using these data, linear, bi-linear and full Goodman diagrams are constructed using mean and “95/95” fits to the data. The various Goodman diagrams are used to predict of failure stress for coupons tested using the WISPERX spectrum [3]. Three models are used in the analyses. The first is the linear Miner’s rule commonly used by the wind industry to predict failure (service lifetimes). The second is a nonlinear variation of Miner’s rule which computes a nonlinear Miner’s Sum based upon an exponential degradation parameter. The third is nonlinear residual strength model that also relies on an exponential degradation parameter. The results illustrate that the Miner’s rule does not predict failure very well. Both nonlinear models predict the experimental data very well when the detailed Goodman is used. Namely, when the mean Goodman diagram is used, the nonlinear models predict failures near the mean of the experimental data and when the 95/95 Goodman diagram is used, they predict the lower bound of the measured data very well.

Keywords: wind, blades, fatigue, spectral, fiberglass.

1 Introduction

In many analyses of wind turbine blades, the effects of

mean stress on the determination of damage in composite blades are either ignored completely or they are characterized inadequately. Mandell, et al [1] have recently presented an updated characterization of the fatigue properties for fiberglass materials that are typically used in wind turbine blades. Their formulation uses the MSU/DOE Fatigue Data Base [2] and a three-parameter model to describe the mean S-N behavior of the fiberglass at thirteen different R-values. The R-value for a fatigue cycle is defined as:

$$R = \frac{\sigma_{\min}}{\sigma_{\max}}, \quad (1)$$

where σ_{\min} is the minimum stress and σ_{\max} is the maximum stress in a fatigue stress cycle (tension is considered positive and compression is negative).

The results are typically presented as a Goodman diagram in which the cycles-to-failure are plotted as a function of mean stress and amplitude along lines of constant R-values. This diagram is the most detailed to date, and it includes several loading conditions that have been poorly represented in earlier studies.

This formulation allows the effects of mean stress on damage calculations to be evaluated. Using field data from the Long term Inflow and Structural Test (LIST) program, Sutherland and Mandell [4] have shown that the updated Goodman diagram predicts longer service lifetimes and lower equivalent fatigue loads than previous analyses. This prediction is a direct result of the lower damage predicted for the high-mean-stress fatigue cycles by the updated Goodman diagram.

To validate this result in a controlled set of experiments, the spectral loading data of Wahl et al [5] is evaluated using the updated Goodman diagram. These coupon data were tested to failure using the WISPERX spectrum [3]. Six formulations for the S-N behavior of fiberglass are used: three using mean fits of the S-N data and three using “95/95” fits. Each set of fits contains the linear, bi-linear and full (13 R-values) Goodman diagrams. When using a Miner’s

¹ *Sandia is a multiprogram laboratory operated by Sandia Corporation, a Lockheed Martin company, for the U.S. Department of Energy under contract DE-AC04-94AL85000

sum, the results illustrate that the mean fits do not predict failure very well, while the 95/95 predicts failures near the mean of measured data. A nonlinear residual strength model is then used to examine another modeling technique. This model when used with the 95/95 Goodman diagram predicts the lower bound of the measured data very well. A nonlinear Miner's sum residual strength model of similar form to the nonlinear model is also shown to predict the lower bound of the measured data very well.

2 Fatigue Data

The DOE/MSU fatigue database² contains over 8800 test results for over 130 material systems [2]. The database contains information on composite materials typically used in wind turbine applications that are constructed from fiberglass and carbon fibers in a variety of matrix materials. References 2, 6 and 7 provide a detailed analysis of data trends and blade substructure applications; substructure applications.

Recent efforts to improve the accuracy of spectrum loading lifetime predictions for fiberglass composites have led to the development of a more complete Goodman diagram than previously available, and a more accurate fatigue model.

2.1 Constant Amplitude Data

The material under consideration here is a typical fiberglass laminate that is called DD-16 in the DOE/MSU Database. This laminate has a [90/0/±45/0]S configuration with a fiber volume fraction of 0.36. The 90° and 0° plies are D155 stitched unidirectional fabric, the ±45° plies are DB120 stitched fabric, and the resin is an orthopolyester. Mandell et al [2, 5] described the test methodologies used to obtain the data cited here. This material has a static tensile strength of 625 MPa and a compressive strength of 400 MPa. The 95/95 strength values are 510 MPa and 357 MPa, respectively. These strength values were determined at a strain rate similar to that of the fatigue tests.

For illustrative purposes, the constant amplitude data at R = -1, 0.1 and 10 are shown in Fig. 1. A complete set of the data for all thirteen R-values is available in Refs. 1 and 2.

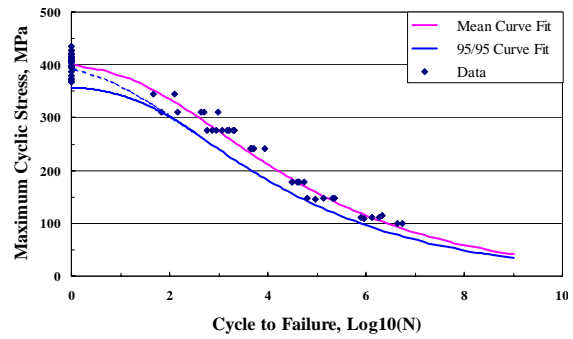


Figure 1a: Data for R= -1.

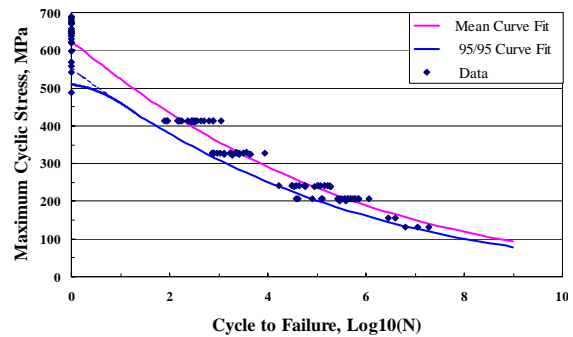


Figure 1b: Data for R=0.1

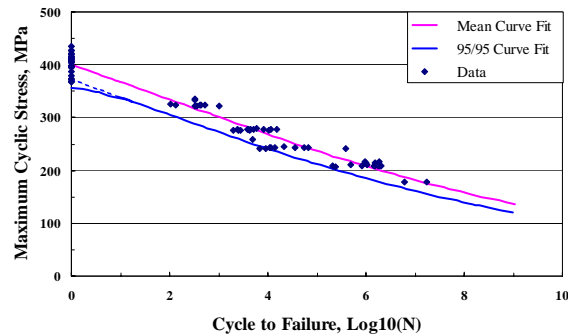


Figure 1c: Data for R= 10

Figure 1: Maximum Absolute Stress versus Cycles to Failure for Thirteen R-Values for Database Material DD16

2.1.1 Curve Fits

2.1.1.1 Mean Fit

As presented by Mandell et al [1], the constant amplitude data at 13 R-values were fit with a three-parameter equation of the following form:

² The database is available on the SNL website: <http://www.sandia.gov/wind/>.

Table I: Parameters for the Thirteen R-Values for Material DD16 and for Small Strands

R-Value	Model (Equation 2)			95/95 (Equation 6)
	a	b	c	$\log_{10}(N_o)$
1.1	0.06	3	0.05	4.43
1.43	0.06	3	0.15	1.85
2	0.06	4	0.25	2.67
10	0.1	4	0.35	0.87
-2	0.01	4	0.55	0.59
-1	0.02	3	0.62	0.53
-0.5	0.45	0.85	0.25	0.64
0.1	0.42	0.58	0.18	0.70
0.5	0.075	2.5	0.43	0.79
0.7	0.04	2.5	0.45	0.65
0.8	0.035	2.5	0.4	0.79
0.9	0.06	2.5	0.28	1.20
1*	0.21	3	0.14	3.03

*Assumes a frequency of 10 Hz.

$$\sigma_o - \sigma = a\sigma \left[\frac{\sigma}{\sigma_o} \right]^b (N^c - 1) \quad , \quad (2)$$

where σ is the maximum applied stress, σ_o is the ultimate tensile or compressive strength (obtained at a strain rate similar to the 10 Hz fatigue tests), and a, b, and c are the fitting parameters. The results of these fits are summarized in Table I and in Fig. 1.

The parameters in these curve fits were selected to provide the best fit to the experimental data and to provide a 10^9 cycle extrapolation stress which was within ten (10) percent of the extrapolation from a simple two-parameter power law fit to the fatigue data having lifetimes greater than 1000 cycles [1].

2.1.1.2 95/95 Fit

Using the techniques cited in Ref. 8 and 9 and the “Standard Practice” cited in Ref. 10, the “95/95” curve fit was also determined for these data. The 95/95 fit implies that, with a 95 percent level of confidence, the material will meet or exceed this design value 95 percent of the time.

For these calculations, we use a one-sided tolerance limit, which has been computed and tabulated for several distributions by a number of authors. Typically, these tabulations take the following form:

$$X^* = \bar{X} - c_{1-\alpha,\gamma} \sigma_x \quad , \quad (3)$$

where the sample average \bar{X} is given by

$$\bar{X} = \frac{\sum_{i=1}^n X_i}{n} \quad . \quad (4)$$

for the ultimate strength data and by Eq. 2 for the fatigue data. $c_{1-\alpha,\gamma}$ is a multiplier (factor) tabulated as a function of the confidence level $(1-\alpha)$, probability γ and the number of data points n. The standard deviation σ_x is given by:

$$\sigma_x = \left[\frac{\sum_{i=1}^n (X_i - \bar{X})^2}{(n-1)} \right]^{\frac{1}{2}} \quad (5)$$

$$= \left[\frac{n \sum_{i=1}^n X_i^2 - \left(\sum_{i=1}^n X_i \right)^2}{n(n-1)} \right]^{\frac{1}{2}} \quad .$$

For these fits, the independent variable X is the number of cycles to failure N. Thus, the number of cycles to failure for the 95/95 fit is given by:

$$\log_{10} [N_{95/95}] = \log_{10} [N] + \log_{10} [N_o] \quad , \quad (6)$$

where N is determined from Eq. 2 and $\log_{10}[N_o]$ is shown in Table I for each of the thirteen R-values.

As shown in Fig. 1, this technique works well for the fatigue data, but in many cases it predicts a 95/95 static strength that is not in agreement with the calculated value (see the dotted line in the figure). To rectify this situation, the 95/95 fatigue curve was “faired” into the measured 95/95 static strength, as shown by the solid lines in the figure [11].

2.1.2 Goodman Diagrams

For the analysis of S-N data, the preferred characterization is the Goodman diagram. In this formulation, the cycles-to-failure are plotted as a function of mean stress and amplitude along lines of constant R-values. Between R-value lines, the constant cycles-to-failure plots are typically, but not always, taken to be straight lines.

Typical Goodman diagrams are shown in Figs. 2 and 3. These figures are presented in increasing level of knowledge about the S-N behavior of the fiberglass composite material. Figures 2a and 3a illustrate the “linear” Goodman diagram. In these figures, the diagrams are constructed using the static strength values for the R = 1 intercept (the horizontal axis of the diagram) and the S-N data for the R = -1 (the

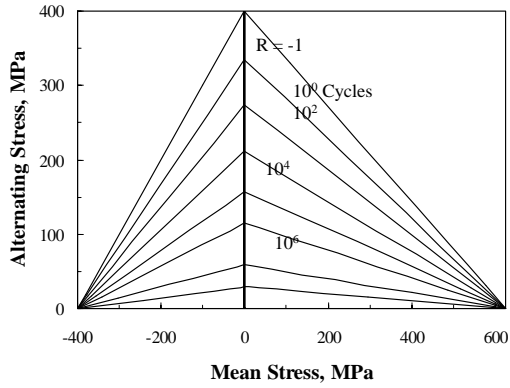


Fig. 2a: Linear Goodman Diagram

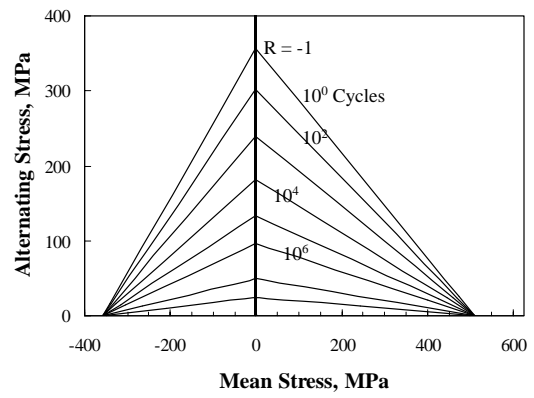


Fig. 3a: Linear Goodman Diagram

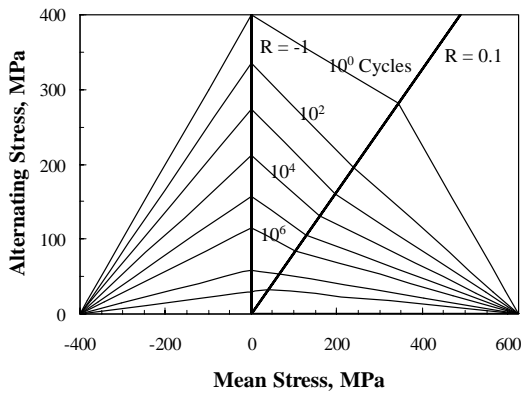


Fig. 2b: Bi-Linear Goodman Diagram

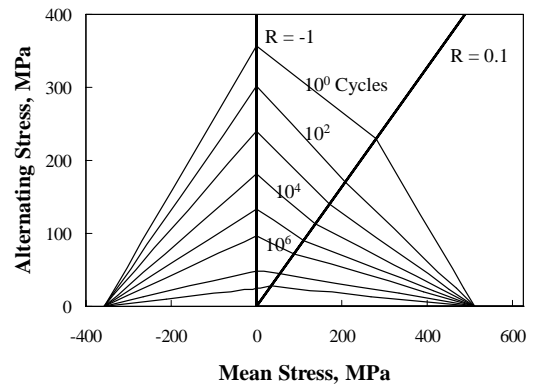


Fig. 3b: Bi-Linear Goodman Diagram

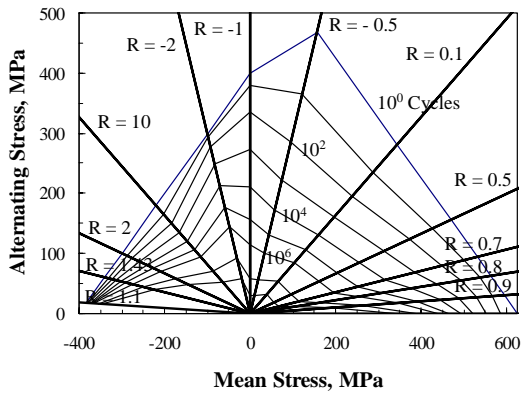


Fig. 2c: Full Goodman Diagram with Thirteen R-Values

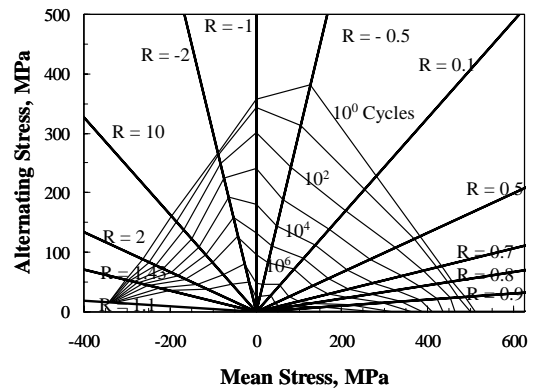


Fig. 3c: Full Goodman Diagram with Thirteen R-Values

Fig. 2. Mean Goodman Diagrams for Database Material DD16, Fit with Eq. 2

Fig. 3. 95/95 Goodman Diagrams for Database Material DD16, Fit with Eqs. 2 and 3

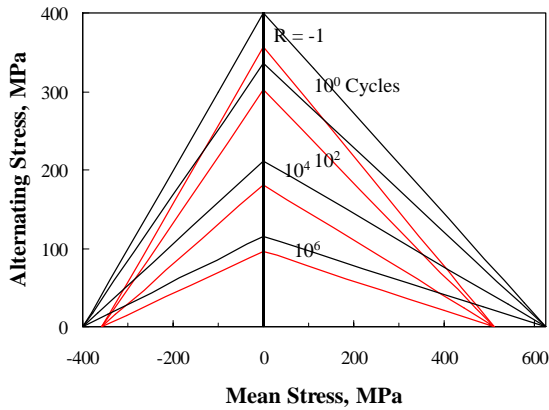


Fig. 4a: Linear Goodman Diagram

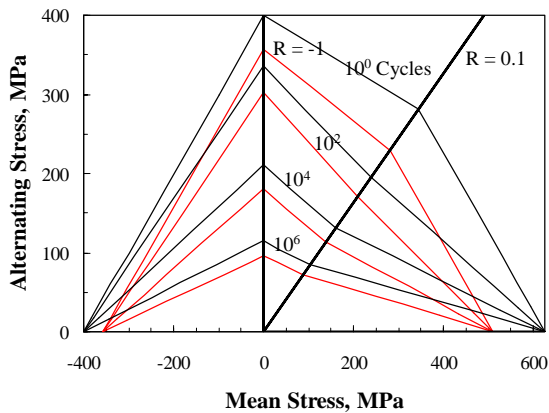


Fig. 4b: Bi-Linear Goodman Diagram

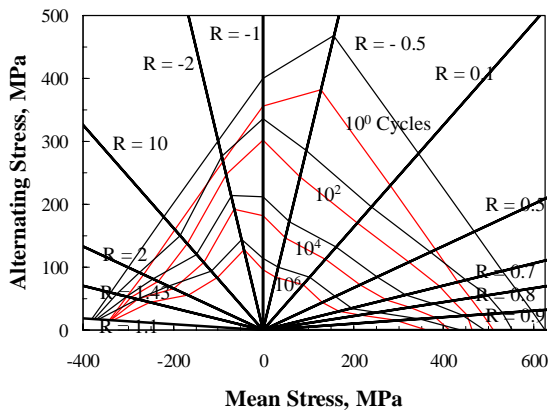


Fig. 4c: MSU/DoE Goodman Diagram for Thirteen R-Values

Fig. 4: Comparison of Mean and 95/95 Goodman Diagrams

vertical axis). The “bi-linear” Goodman diagrams, shown in Figs. 2b and 3b, add the $R = 0.1$ S-N data to the diagram. The “full” Goodman diagrams, shown in Figs. 2c and 3c, add the information the S-N data from the remaining 12 R-values.

2.1.2.1 Mean Goodman Diagrams

The Goodman diagrams cited in Fig. 2 were constructed using Eq. 2 and the information in Table I. Figures 2a and 2b, use the mean static strengths for the intercepts of the constant-life curves with mean (horizontal) axis. Fig. 2c departs from traditional formulations in that the intercept for tensile mean axis ($R = 1$) is not the mean static strength. Rather, the intercept is a range of values based upon time-to-failure under constant load. These data were converted to cycles by assuming a frequency of 10 cycles/second, typical of the cyclic tests. Nijssen et al [12] have hypothesized a similar formulation previously.

2.1.2.2 95/95

The Goodman diagrams cited in Fig. 3 were constructed using Eqs. 2 and 3, the information in Table I, and the fairing of the S-N curves into the 95/95 static strengths. Again, the tensile intercept in Fig. 3c is a range of values based upon time under load.

2.1.2.3 Comparison

The Goodman diagrams presented in Figs. 2 and 3 are compared with one another in Fig. 4. As shown in this figure, the shapes of the various Goodman diagrams are unchanged by their conversion from the mean values to the 95/95 values.

The significant differences in the Goodman formulations are highlighted in Fig. 5. The area near the $R = -1$ axis is very important because this is the region where the fiberglass composite is in transition between compressive and tensile failure modes and many of the stress cycles on a wind turbine blade have an R-value near -1 . The effect of the mode change on fatigue properties is illustrated by the direct comparison of the constant life curves for the three Goodman diagrams. In this figure, the constant life curves for the three formulations of the Goodman diagram at 10^5 cycles are compared to one another. Four distinct regions of comparison are noted: (1) the region of relatively high compressive mean stress (to the left of $R = 10$); (2) the region of relatively low compressive stress (between $R = 10$ and $R = -1$); (3) the region of relatively low tensile stress (between $R = -1$ and $R = 0.1$); and (4) the region of relatively high tensile stress (to the right of $R = 0.1$). In the first and third regions, the three formulations lie close to one

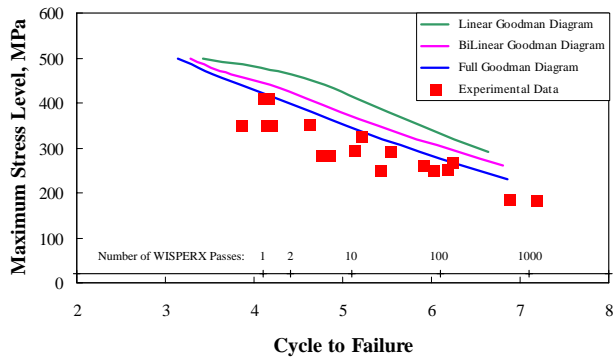


Fig. 7a: Mean Goodman Diagram

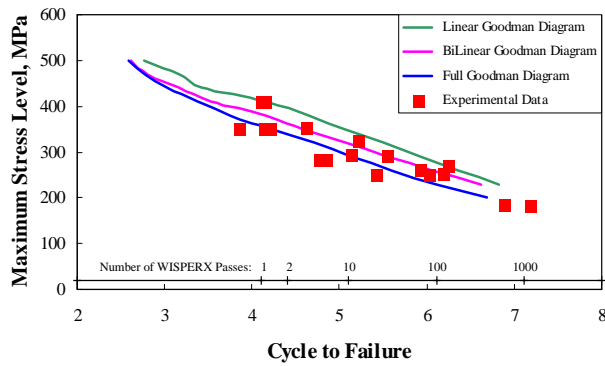


Fig. 7b: 95/95 Goodman Diagram

Fig. 7: Comparison of Experimental Data to Predicted Failure using Linear Miner's Rule

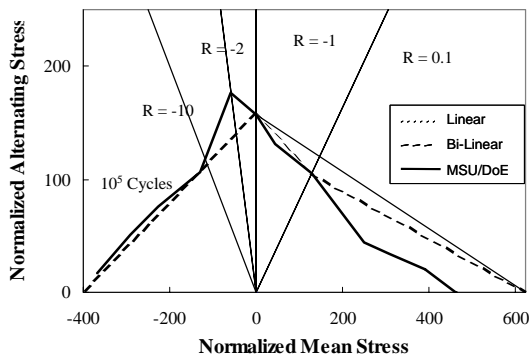


Fig. 5: Comparison of the Three Goodman Diagram at 10^5 Cycles

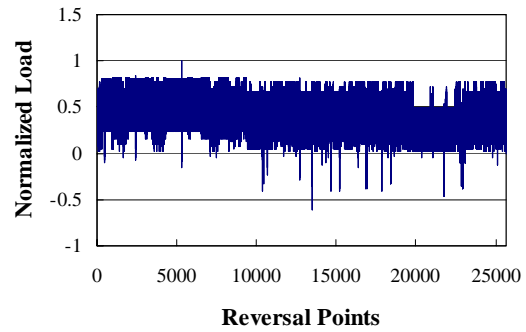


Fig. 6: Normalized WISPERX Spectrum

another. Thus, each of the three formulations will predict approximately the same damage rate for the stress cycles in this range. For the fourth region (high tensile stress) the database formulation is below the linear and bi-linear formulations. Thus, the database formulation is more severe (i.e., shorter predicted service lifetime) than the other two. And, finally, for the second region (low compressive stress), the database formulation is above the linear and bi-linear formulations. Thus, it is less severe. Regions 2 and 3 are where the composite is in transition between compressive and tensile failure modes.

2.2 WISPERX Spectral Data

Wahl et al [5] have conducted spectral loading tests of coupons using the WISPERX spectrum [3]. The WISPERX spectrum is the WISPER spectrum with the small amplitude fatigue cycles removed. The spectrum, see Fig. 6, consists of over 25,000 peaks-and-valleys (load reversal points). The original formulation of the spectrum is in terms of load levels that vary from 0 to 64 with zero at load level 25. For testing the load levels were changed to the normalized form shown in the figure. In this form, the load at each reversal is ratioed to the maximum load. Thus, the test spectrum is a simple multiple of these reversal points by the maximum load in the spectrum. In this form, the maximum load in the spectrum is 1.0 and the minimum is -0.6923 .

The experimental cycles-to-failure as a function of the maximum stress in the spectrum for material DD16 are shown in Fig. 7 [5].

3 Damage Models

Typically, the wind industry uses Miner's rule to estimate damage under spectral loads. Many other models for damage estimation have been proposed. Two, which are investigated here, are the nonlinear Miner's Sum proposed by Hwang et al [13] and the nonlinear residual strength model proposed by Yang et al [14]. A complete description of these models is provided by Wahl et al [5].

3.1 Miner's Rule

Miner's rule defines the damage \mathbf{D} , predicted for a time interval T , as

$$\mathbf{D} = \sum_i \frac{n_i(\sigma)}{N_i(\sigma)} \quad , \quad (7)$$

where n is the number-of-cycles, N is the number-of-cycles to failure and σ describes the stress level of fatigue cycle. For our case where we will be using the Goodman diagrams to determine N , σ is divided into two components: the mean stress of σ_m and the amplitude of σ_A of the stress cycle.

Failure occurs when \mathbf{D} equals one. The predicted service lifetime \mathbf{L} , is the time T required for the damage \mathbf{D} (T) to accumulate to a value of one.

3.2 Residual Strength Models

3.2.1 Miner's Sum Nonlinear Model

Miner's rule may also be used to describe the residual strength of composites, see discussion by Wahl et al [5]. In its general form, the nonlinear Miner's sum model has the following form:

$$\left[\frac{\sigma_R}{\sigma_o} \right]_i = 1 - \sum_{j=1}^i \left[\frac{n_j}{N_j} \right]^v \quad , \quad (8)$$

where $[\sigma_R/\sigma_o]$ is the ratio of the residual strength to the static strength σ_o after step i and the exponent v is the nonlinear degradation parameter. As discussed above, N_j is evaluated at their implied stress state (σ_m , σ_A) of n_j .

3.2.2 Generalized Nonlinear Model

A generalized nonlinear residual strength model, see discussion by Wahl et al [5], takes the form:

$$\left[\frac{\sigma_R}{\sigma_o} \right]_i = \left[\frac{\sigma_i - \sigma_o}{\sigma_o} \right] \left[\frac{n_i + (n_{i-1})^*}{N_i(\sigma_m, \sigma_A)} \right]^v \quad , \quad (9)$$

where n_i is the current number of stress cycles and $(n_{i-1})^*$ is the number of previous equivalent cycles

determined for the current stress level. The previous equivalent cycles is the number of cycles which would give the residual stress ratio $[\sigma_R/\sigma_o]_i$ if cycled only at (σ_m , σ_A).

If Eq. 9 is rewritten as:

$$\left[\frac{\sigma_R}{\sigma_o} \right]_i = \left[\frac{\sigma_i - \sigma_o}{\sigma_o} \right] \left[\frac{1}{N_i(\sigma_i, R)} \right]^v \left[n_i + (n_{i-1})^* \right]^v \quad , \quad (10)$$

$$= A_i \left[n_i + (n_{i-1})^* \right]^v$$

then,

$$A_i \left[(n_{i-1})^* \right]^v = A_{i-1} \left[(n_{i-1}) \right]^v \quad , \quad \text{or} \quad (11)$$

$$(n_{i-1})^* = \left[\frac{A_{i-1}}{A_i} \right]^{1/v} (n_{i-1}) \quad . \quad (12)$$

For this analysis, we have computed the residual strength sequentially using Eqs. 9 through 12 for each half-cycle of the sequence.

3.2.3 Residual Strength Ratio

As defined by Eqs. 8 and 10, the residual strength of the composite after i steps for both residual strength models is

$$(\sigma_R)_{i+1} = \left[\frac{\sigma_R}{\sigma_o} \right]_i (\sigma_o)_i \quad . \quad (13)$$

Failure occurs when:

$$\sigma_i \geq (\sigma_R)_i \quad . \quad (14)$$

While Eq. 13 is rather obvious, this equation implies that the residual tensile and compressive strength are being reduced proportionally.

In this form, the ratio of the residual stress to the static strength is a monotonically decreasing function. As the static strength σ_o may equal either the tensile or the compressive strength (depending on the R -value of the i^{th} cycle), the absolute value of the residual strength is not a monotonically decreasing function.

4 Damage Predictions

The models cited in Section 3 are used here to predict the failures of the coupons tested under the WISPERX load spectrum that are cited in Section 2.

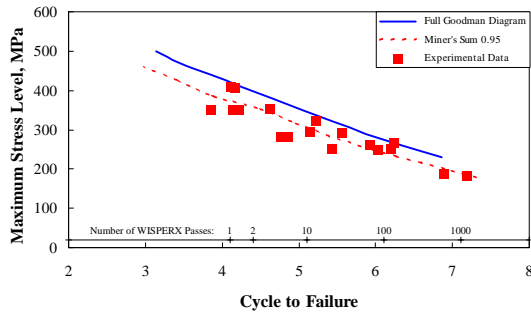


Fig. 8a: Mean Goodman Diagram

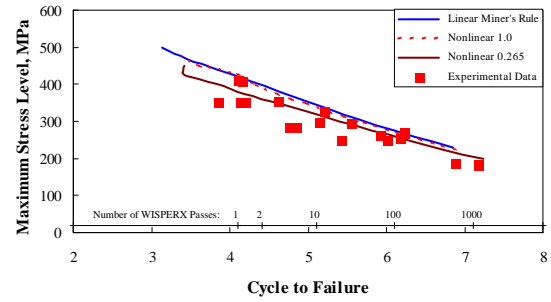


Fig. 9a: Mean Goodman Diagram

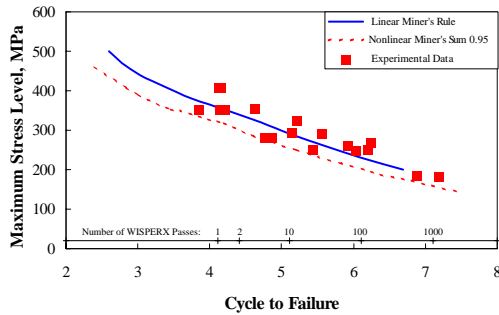


Fig. 8b: 95/95 Goodman Diagram

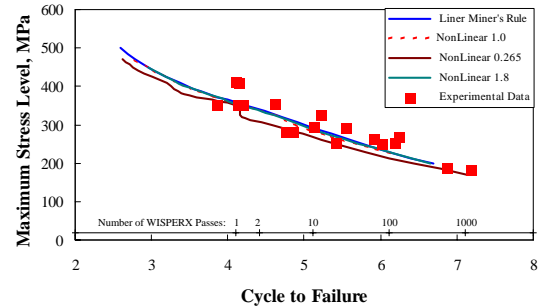


Fig. 9b: 95/95 Goodman Diagram

Fig. 8: Comparison of Experimental Data to Predicted Failure using NonLinear Miner's Sum Residual Strength Models

Fig. 9: Comparison of Experimental Data to Predicted Failure using Nonlinear Residual Strength Models

4.1 Miner's Rule

The predictions for Miner's rule using the three mean-value Goodman diagrams (see Fig. 2) are shown in Fig. 7a. The linear Goodman diagram predicts the longest lifetimes (cycles-to-failure) and the full Goodman diagram predicts the shortest lifetimes. This comparison illustrates that the mean fits do not pass through the mean of the data. Rather, all three formulations predict service lifetimes that are significantly higher than the measured lifetime.

The predictions for Miner's rule using the three 95/95 Goodman diagrams (see Fig. 3) are shown in Fig. 7b. Again, the linear Goodman diagram predicts the longest lifetimes (cycles-to-failure) and the full Goodman diagram predicts the shortest lifetimes. This comparison illustrates that the linear 95/95 Goodman diagram predicts service lifetimes that are higher than the measured lifetime. And, the full 95/95 Goodman diagram predicts lifetimes near the mean of the experimental data.

Thus, Miner's rule does not predict the measured lifetimes very well. And, even the 95/95 Goodman

diagrams are non-conservative in that they predict longer service lifetimes than those measured in the tests using the WISPERX load spectrum. At best, the full 95/95 Goodman diagram predicts the mean of measured data.

4.2 Residual Strength Models

The predicted lifetimes for spectral loading using the WISPERX spectrum are summarized in Figs. 8 and 9.

4.2.1 Nonlinear Miner's Sum Model

Noting that in Fig. 7, the slopes of the predicted lifetime curves are consistent with the data, but they are shifted to the right of the data. The nonlinear Miner's Sum model described in Eq. 8 shifts the prediction to the left when the exponent ν is taken to be less than one. Using a trial-and-error method, a value of $\nu = 0.95$ was chosen as the best fit to the experientially measured lifetime data using the 95/95 Goodman diagram. The predictions for the linear residual strength model are shown in Fig. 8.

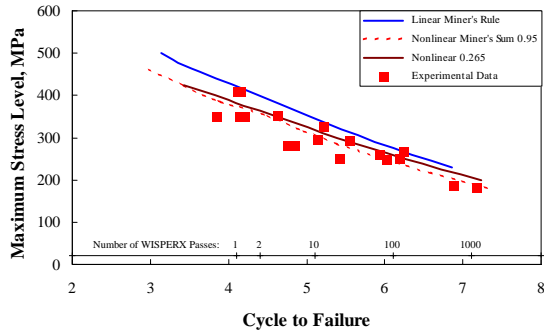


Fig. 10a: Mean Goodman Diagram

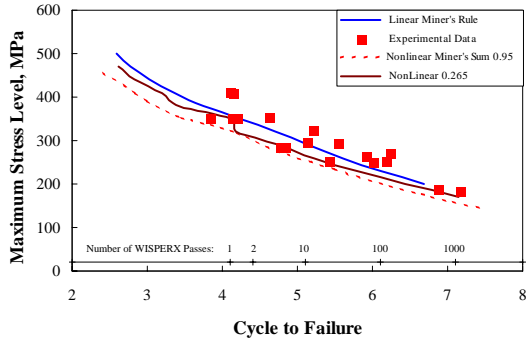


Fig. 10b: 95/95 Goodman Diagram

Fig. 10: Comparison of Experimental Data to Predicted Failure using NonLinear Miner's Sum Residual Strength Models

As shown in this figure, the lifetime curve predicted by Miner's rule has been shifted to the left by approximately a half-decade of cycles by the linear residual strength model. The predictions are in very good agreement with the measured lifetimes. Namely, the predicted lifetimes are near the mean of the data in Fig. 9a and at or below the measured lifetimes in Fig. 9b.

4.2.2 Nonlinear Residual Strength Model

The predictions for the nonlinear residual strength model using the full and the 95/95 Goodman diagram (see Fig. 3c and 4c) are shown in Fig. 9. These data were used to determine an appropriate value for the nonlinear degradation exponent ν . As shown in this figure, for $\nu = 1$, the prediction lies on top of the 95/95 Goodman Miner's rule prediction. For illustrative purposes, a $\nu = 1.8$ was also shown in Fig. 9b. The predictions for this value of ν also lies on top of the 95/95 Goodman Miner's rule prediction.

Using the value chosen by Wahl et al [5] of $\nu = 0.265$, the predictions are in general agreement with the data.

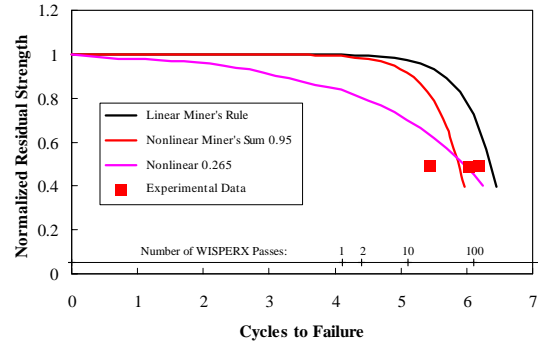


Fig. 11a: Mean Goodman Diagram

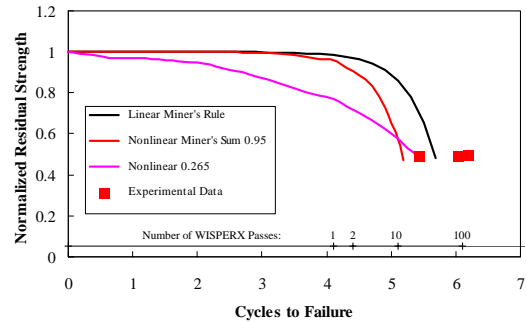


Fig. 11b: 95/95 Goodman Diagram

Fig. 11: Comparison of Experimental Data to Predicted Failure using the Nonlinear Residual Strength Model at a Maximum Load Level of 250 MPa

Namely, the predicted lifetimes are near the mean of the data in Fig. 9a and at or below the measured lifetimes in Fig. 9b. Thus, the nonlinear model with an exponent of 0.265 is a good predictor of the measured lifetime when used with the full Goodman diagram.

The step in the predicted lifetime at approximately 400 MPa and 10^4 cycles is a direct result of the WISPERX spectrum. As shown in Fig. 6, this load spectrum contains one very large tension cycle after approximately 5000 cycles. This cycle is the cause of failure at both levels of the cited step. Namely, the residual strength is progressively decreasing, until it encounters this very large cycle. This cycle exceeds the current residual strength of the composite and failure insures.

4.2.3 Residual Strength Comparisons

Figures 10 and 11 illustrate the predicted residual failure strength of the composite using the linear Miner's rule and the two nonlinear residual strength models.

The major difference between the three models is illustrated in Fig. 11. As shown in this figure, the loss of residual strength as fatigue cycles accumulate is very different. For Miner's rule, the composite retains its strength for most of its lifetime, and, as failure approaches, its residual strength drops precipitously. For the nonlinear Miner's sum with $\nu = 0.95$, the residual strength curve maintains the same form, but is shifted to the left, i.e., a shorter lifetime. For the nonlinear residual strength model with $\nu = 0.265$, the residual strength starts decreasing almost immediately and continues to decrease until failure occurs. Also illustrated in this figure is the ability of both nonlinear residual strength models to predict the measured lifetime of the composite at this load level, i.e. at a maximum load level of 250 MPa.

5 Concluding Remarks

The updated Goodman diagrams presented here have been developed using the MSU/DOE Fatigue Data Base [2]. The diagram is based upon S-N data obtained at thirteen different R-values. Separate Goodman diagrams were constructed using both the mean and the 95/95 representations of the data. The effects of these improved representations of fiberglass composite behavior were illustrated using coupons tested to failure using the WISPERX load spectrum [3]. These comparisons illustrate that when a Miner's rule damage criterion is used, the mean fits of the data do not predict failure very well, while the 95/95 predicts failures near the mean of measured data. Both a nonlinear Miner's sum model and a nonlinear residual strength model used with the 95/95 Goodman diagram predicts the lower bound of the measured data very well and when used with the mean Goodman diagram, the nonlinear models also predict the mean lifetime very well.

6 References

- [1] Mandell, J.F., D.D. Samborsky, N.K. Wahl, and H.J. Sutherland, "Testing and Analysis of Low Cost Composite Materials Under Spectrum Loading and High Cycle Fatigue Conditions," Conference Paper, *ICCM14*, Paper # 1811, SME/ASC, 2003.
- [2] Mandell, J.F., and D.D. Samborsky, *DOE/MSU Composite Material Fatigue Database: Test Methods, Materials, and Analysis*, Report SAND97-3002, Sandia National Laboratories, Albuquerque, NM, 1997.
- [3]. Ten Have, A.A., *WISPER and WISPERX: Final Definition of Two Standardized Fatigue Loading Sequences for Wind Turbine Blades*, NLR-TP-91476U, National Aerospace Laboratory NLR, Amsterdam, the Netherlands, 1992,
- [4]. Sutherland, H.J., and J.F. Mandell, "Effect of Mean Stress on the Damage of Wind Turbine Blades," *2004 ASME Wind Energy Symposium*, AIAA/ASME, 2004.
- [5] Wahl, N.K., J.F. Mandell, D.D. Samborsky, *Spectrum Fatigue Lifetime and Residual Strength for Fiberglass Laminates*, Report SAND2002-0546, Sandia National Laboratories, Albuquerque, NM, 2002.
- [6] Mandell, J.F., D.D. Samborsky, and D.S. Cairns, *Fatigue of Composite Materials and Substructures for Wind Turbine Blade*, Contractor Report SAND2002-077, Sandia National Laboratories, Albuquerque, NM, 2002.
- [7] Mandell, J.F., D.D. Samborsky, D.W. Combs, M.E. Scott and D.S. Cairns, *Fatigue of Composite Material Beam Elements Representative of Wind Turbine Blade Substructure*, Report NREL/SR-500-24374, National Renewable Energy Laboratory, Golden, Co, 1998.
- [8] Echtermeyer, T., E. Hayman, and K.O. Ronold, "Estimation of Fatigue Curves for Design of Composite Laminates," *Composites-Part A (Applied Science and Manufacturing)*, Vol. 27A, No. 6, 1996, p. 485.
- [9] Sutherland, H.J., and P.S. Veers, "The Development of Confidence Limits For Fatigue Strength Data," *2000 ASME Wind Energy Symposium*, AIAA/ASME, 2000, pp. 413-423.
- [10] ASTM, E739-91, *Standard Practice for Statistical Analysis of Linear or Linearized Stress-Life (S-N) and Strain-Life (e-N) Fatigue Data*, ASTM, Conshohocken, PA.
- [11] Kensche, C.W., "Effects of Environment," *Design of Composite Structures Against Fatigue*, R. M. Mayer, ed., Mechanical Engineering Pub. Limited, Bury St Edmunds, Suffolk, UK, 1996, pp.65-87
- [12] Nijssen, R.P.L, D.R.V. van Delft and A.M. van Wingerde, "Alternative Fatigue Lifetime Prediction Formulations for variable Amplitude Loading," *2002 ASME Wind Energy Symposium*, AIAA/ASME, pp. 10-18.
- [13] Hwang, W., and K.S. Han, "Cumulative Damage Models and Multi-Stress Fatigue Life Prediction," *J. of Composite Materials*, Vol. 20, March, 1986, pp. 125-153.
- [14] Yang, J.N., D.L. Jones, S.H. Yang, and A. Meskini, "A Stiffness Degradation Model for Graphite/Epoxy Laminates," *J. of Composite Materials*, Vol. 24, July, 1990, pp. 753-769.